RESEARCH PAPER

OncoImmunology 1:6, 829–839; September 2012; © 2012 Landes Bioscience

High endothelial venules (HEVs) in human melanoma lesions

Major gateways for tumor-infiltrating lymphocytes

Ludovic Martinet,[1,2,3] Sophie Le Guellec,[3] Thomas Filleron,[3] Laurence Lamant,[2,4,5] Nicolas Meyer,[5] Philippe Rochaix,[3] Ignacio Garrido[1,2,3,5] and Jean-Philippe Girard[1,2,*]

[1]CNRS; IPBS (Institut de Pharmacologie et de Biologie Structurale); Toulouse, France; [2]Université de Toulouse; Toulouse, France; [3]Institut Claudius Regaud; Toulouse, France; [4]Centre de Recherches en Cancerologie de Toulouse; Toulouse, France; [5]CHU de Toulouse; Toulouse, France

Keywords: tumor-infiltrating lymphocytes, blood vessels, melanoma, immunity, chemokine, dendritic cells

The presence of tumor-infiltrating lymphocytes (TILs) is a strong prognostic parameter for local dissemination and overall survival in melanoma. Lymphocyte migration from blood into peripheral tissues is mainly regulated by vascular endothelium. However, the blood vessels and mechanisms governing the recruitment of TILs in melanoma tumors remain poorly understood. Here, we show that high endothelial venules (HEVs), specialized blood vessels for lymphocyte extravasation into lymphoid tissues, are frequently found in melanoma tumors and are associated with high levels of lymphocyte infiltration. The analysis of 225 primary melanomas revealed that lymphocytes specifically infiltrated HEV-rich areas of melanoma tumors and that the density of MECA-79$^+$ HEVs was variable among patients and strongly correlated with CD3$^+$, CD8$^+$ and CD20$^+$ TIL densities. Inflammatory (*CCL5*, *CXCL9*, *CXCL10* and *CXCL11*) and lymphoid (*CCL21*, *CCL19* and *CXCL13*) chemokines as well as T_H1 and naïve T-cell genes were overexpressed in melanoma samples with high densities of tumor HEVs. Mature dendritic cells (mDCs) were frequently found around tumor HEVs and densities of HEVs and DC-LAMP$^+$ mDCs within tumor stroma were strongly correlated. DCs which maintain HEVs in lymph nodes, may thus also contribute to the regulation of HEVs in melanomas. Finally, we found significantly higher densities of tumor HEVs in melanomas with tumor regression, low Clark level of invasion and thin Breslow thickness (all $p < 0.001$). The strong association between tumor HEVs, TILs, mDCs and clinical parameters of melanoma, supports a critical role for HEVs in limiting malignant melanoma development through both naïve and effector T-lymphocyte recruitment and activation.

Introduction

The incidence of metastatic melanoma has increased over the past three decades and the death rate continues to rise faster than the rate of most other cancers. The World Health Organization estimates that there are 66,000 deaths from skin cancer annually worldwide, with approximately 80% due to melanoma. Although primary cutaneous melanoma is curable in its early stages with surgical resection, patients with metastatic melanoma have a median survival of less than 1 y.[1]

Immunological factors have been shown to constitute a major predictor of good clinical outcome in solid cancers, including breast, colorectal and ovarian carcinomas.[2-6] The presence of tumor-infiltrating lymphocytes (TILs) in primary cutaneous melanomas is also a strong prognostic parameter for lymph node dissemination[7] and overall survival.[8,9] Further implication of the immune system in melanoma come from a recent phase III study showing that monoclonal antibody *Ipilimumab*, targeting T-cell inhibitory receptor CTLA-4, improved overall survival in patients with metastatic melanoma.[10] Even if immune-based therapies have led to progress in the treatment of metastatic melanoma,[11-13] tumor infiltration by activated lymphocytes is a current frontier to successful cancer therapy.[14]

Lymphocyte migration from blood circulation into peripheral tissues is regulated by vascular endothelium.[15] However, blood vessels and mechanisms governing the recruitment of lymphocytes into melanoma remain poorly understood. Evidence has recently been provided that cancer development can alter blood vessel function and restrict lymphocyte infiltration into tumors.[16,17] In contrast, the characteristics of tumor blood vessels that facilitate large scale influx of lymphocytes within human melanoma lesions are presently unknown.

High endothelial venules (HEVs) are specialized blood vessels mediating lymphocyte extravasation in lymphoid organs and chronically inflamed tissues.[15,18-20] HEV endothelial cells express high levels of 6-sulfo sialyl Lewis X ligands, recognized by the HEV-specific antibody MECA-79, which mediate the initial capture and rolling of lymphocytes along the HEV vessel wall. Recently, we reported the frequent presence of HEVs in human solid tumors.[21] In a retrospective cohort of 146 invasive breast cancer patients, we found that high densities of tumor HEVs

*Correspondence to: Jean-Philippe Girard; Email: Jean-Philippe.Girard@ipbs.fr
Submitted: 04/11/12; Revised: 04/20/12; Accepted: 04/23/12
http://dx.doi.org/10.4161/onci.20492

were associated with T- and B-lymphocyte infiltration and significantly correlated with longer metastasis-free, disease-free and overall survival rates. However, the impact of tumor HEVs on lymphocyte infiltration and prognosis in melanoma remained to be determined.

In this study, we demonstrate that the density of tumor HEVs is variable among the 225 primary melanomas analyzed and inversely correlated with Breslow thickness and Clark level of invasion. We show that $CD3^+$ and $CD8^+$ T lymphocytes specifically infiltrate HEV-rich areas of melanomas and that lymphocyte infiltration in melanomas is correlated with the density of tumor HEVs. Together, these results suggest that tumor HEVs represent major gateways for lymphocyte infiltration into human melanoma lesions.

Results

Human melanomas contain variable numbers of HEV blood vessels. In order to analyze the presence of HEVs in melanoma, we performed immunohistochemistry with the HEV-specific antibody MECA-79 on tumor sections from a cohort of 225 patients operated for a primary melanoma between 2000 and 2012. Absolute numbers of MECA-79^+ vessels present within the tumor area were quantified and the density of tumor HEVs (HEV/mm^2) was calculated for each patient (**Fig. 1A**). MECA-79^+ blood vessels were detected in almost two-thirds of the tumors analyzed (n = 152/225). In contrast, MECA-79^+ vessels were never detected in normal skin samples distant from the tumor site (**Fig. S1**). The number of MECA-79^+ HEVs detected within the tumor stroma was highly heterogeneous among the different melanomas ranging from 0 to 201 HEVs per tumor section with a median and a mean value of 6.5 and 24.7 HEVs per tumor section respectively (**Fig. 1B**). The density of HEVs within the tumor stroma was also highly variable among patients ranging from 0 to 27.2 HEVs/mm^2 with a median and a mean value of 0.81 and 3.1 HEVs/mm^2 respectively (**Fig. 1B**).

To further characterize the phenotype of tumor HEVs found in the stroma of human melanomas, we performed immunofluorescence staining against several blood vessel markers (CD31, vWB and DARC) and HEV markers (HECA452, G72 and G152). These analyses revealed that the endothelial cells of melanoma tumor HEVs display a plump morphology, express pan-vascular endothelial cells markers CD31 and vWB, post-capillary veinule marker DARC and strongly react with HECA-452, G72 and G152 antibodies that recognize 6-sulfo sialyl Lewis X ligands for lymphocytes (**Fig. 1C**). Therefore, MECA-79^+ HEVs found in human melanomas have the bona fide phenotype of HEV blood vessels.

The density of tumor HEVs correlates with clinical parameters of melanoma. We analyzed the clinical characteristics and prognostic factors of primary melanoma of our cohort according to the density of tumor HEVs (**Table 1**). We found no significant correlations between HEV densities and the age or sex of patients. In contrast, significant differences in the density of tumor HEVs were observed between different anatomic sites and melanoma histologic types (**Table 1**). The highest density of tumor HEVs was found in Dubreuilh melanoma followed by superficial spreading melanoma (SSM) whereas acral-lentiginous melanoma had the lowest HEV density (**Fig. 2A**). The density of HEVs was also significantly higher in melanomas showing signs of tumor regression (**Fig. 2B**). Breslow tumor thickness is the most powerful prognostic biomarker for staging primary cutaneous melanoma together with ulceration and lymph node involvement.[22] Whereas no significant correlation was observed between HEV density and the presence of tumor ulceration or lymph node invasion (**Table 1**), the density of tumor HEVs was inversely correlated with Breslow thickness (Spearman $r = -0.26$ $p < 0.001$). Among patients with thin lesions (Breslow ≤ 1 mm) the density of HEVs was significantly higher compared with patients with intermediate (Breslow 1.01–2 mm) and thick lesions (Breslow > 2 mm) (**Fig. 2C and Table 1**). Finally, we found significant differences between the density of HEVs and Clark levels of invasion now recommended for staging thin melanomas when mitotic rate is not available.[22] Patients with low Clark levels (I–II) had a significantly higher density of HEVs than patients with intermediate (III) and high Clark levels (IV–V) (**Fig. 2D and Table 1**). Altogether, these results showing that a high density of HEVs is associated with thin melanomas, low levels of invasion and signs of regression suggest that HEV density represents a favorable prognostic biomarker for malignant melanoma.

The density of tumor HEVs predicts lymphocyte infiltration in human melanomas. We observed that lymphoid infiltrates were always located around HEV-rich areas of melanomas suggesting an active role of these vessels in recruitment of TILs (**Fig. 3A**). Immunofluorescence staining revealed that immune cells around tumor HEVs were mainly $CD3^+$ T lymphocytes (**Fig. 3B and C**) and to a lesser extent $CD20^+$ B lymphocytes (**Fig. 3D**). A considerable fraction of $CD3^+$ T lymphocytes were $CD8^+$ cytotoxic T lymphocytes (**Fig. 3E**).

To better define the link between HEVs and TILs in melanoma, we performed immunohistochemistry against $CD3^+$ T cells, $CD8^+$ cytotoxic T cells and $CD20^+$ B cells on serial tumor sections (**Fig. 4A**). For each patient of our melanoma cohort, we quantified $CD3^+$ T cells, $CD8^+$ T cells and $CD20^+$ B cells using semi-quantitative optical grading as previously described in reference 9 (grade 1: absent-low, grade 2: moderate, grade 3: high density of TILs). We observed that the density of tumor HEVs was highly correlated with the density of $CD3^+$ (Spearman $r = 0.71$ $p < 0.0001$) and $CD8^+$ (Spearman $r = 0.67$ $p < 0.0001$) T lymphocytes infiltrating melanomas (**Table S1**). In melanoma with high densities of $CD3^+$ and $CD8^+$ TILs (grade 3), the density of HEVs was significantly higher than in tumors with moderate (grade 2) or low (grade 1) densities of $CD3^+$ or $CD8^+$ TILs (**Fig. 4B**). In accordance with these results, most melanomas that did not contain HEVs (HEV^-) were poorly infiltrated by $CD3^+$ or $CD8^+$ T cells as compared with melanomas with HEVs (HEV^+) (**Fig. S2**). The density of HEVs was also correlated with the density of $CD20^+$ B lymphocytes infiltrating melanomas (Spearman $r = 0.56$ $p < 0.0001$; **Fig. 4B**), although this population represents a smaller fraction of TILs (**Fig. 3D; Fig. S2**). These results, together with the immunofluorescence staining data showing that HEV blood vessels are specifically located

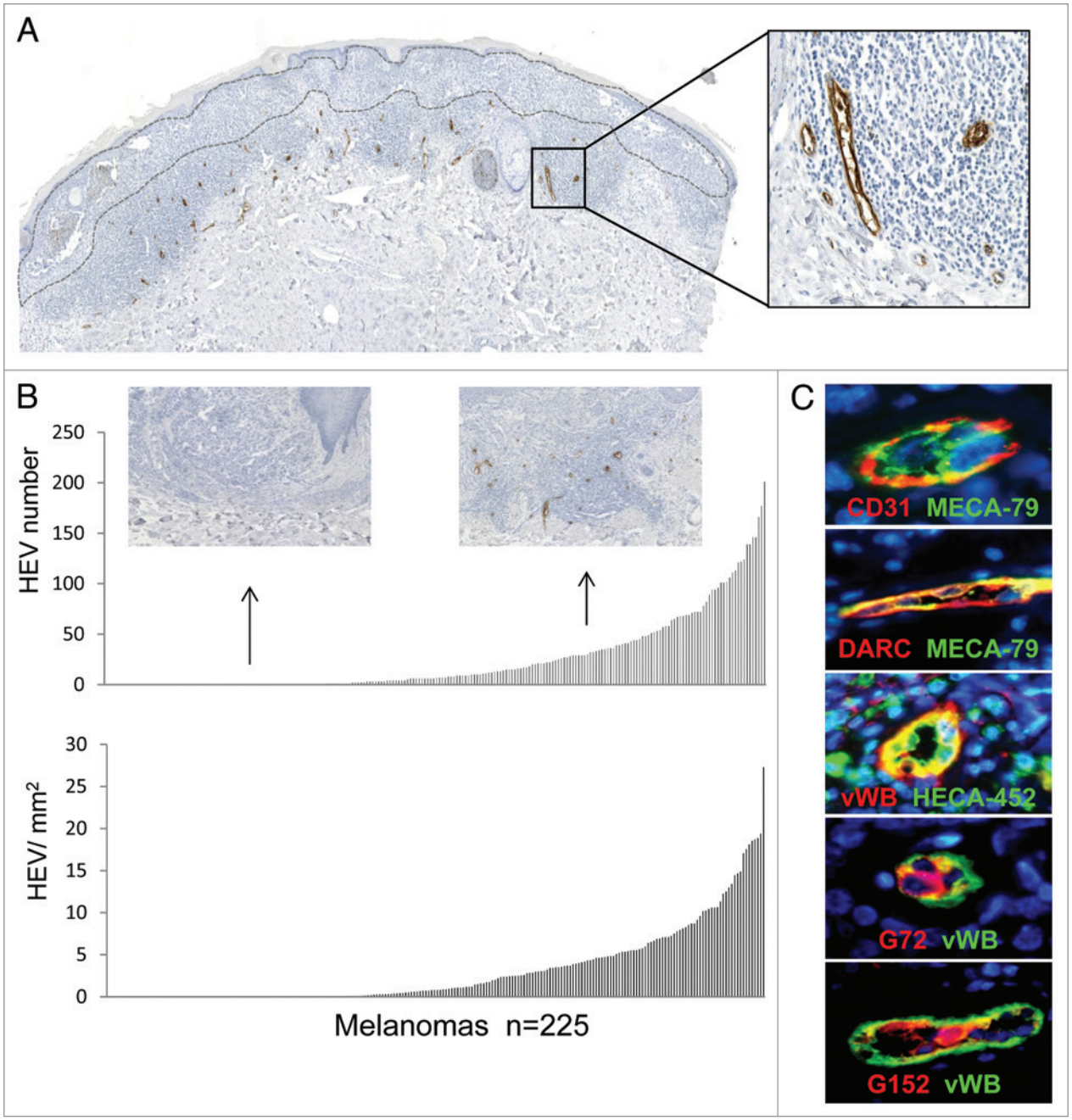

Figure 1. Human melanomas contain variable numbers of HEV blood vessels. (**A**) Representative picture from a digitized tumor slide stained with MECA-79 antibody showing numerous HEV blood vessels located at the invasive front of a melanoma lesion (dashed area). (**B**) Histograms showing the absolute number and the density of MECA-79$^+$ HEVs in the tumor area quantified for 225 primary melanomas. Two representative pictures of melanomas with high and low numbers of MECA-79$^+$ HEVs are shown. (**C**) Phenotypic characterization of tumor HEVs. Tumor HEVs express pan-endothelial cell markers CD31 and vWB, post-capillary venule-specific marker DARC and HEV-specific markers MECA-79, HECA-452, G72 and G152. Immunofluorescence staining of melanoma tumor sections was performed with the indicated antibodies. Counterstaining was performed with DAPI.

within lymphocyte-rich tumor areas, suggest that tumor HEVs are major gateways for lymphocyte infiltration into human melanomas.

We previously described a similar association between the density of tumor HEVs and TILs in breast cancer using a cohort of 146 invasive ductal carcinomas.[21] Comparison of HEVs densities between melanomas and breast tumors revealed that the mean HEV density was more than 10-fold higher in melanomas (3.13 ± 0.31) than in breast tumors (0.24 ± 0.05) (**Fig. 4C**). Similar to the HEV density, the mean density of CD3$^+$ T cells was 10-fold higher in melanomas (3037.0 ± 746.1) than in breast tumors (366.2 ± 45.0) (**Fig. 4C**).

Tumor HEVs have no influence on Foxp3$^+$ regulatory T-cell infiltration in melanoma tumors. Foxp3$^+$ regulatory T cells

Table 1. Characteristics of patients with melanomas (n = 225) according to HEV density

	N	%	Median	HEV/mm² (Range)	P
Age					
< 60 ans	97	(43.1%)	0.7	(0.0:18.9)	p = 0.32
> 60 ans	128	(56.9%)	0.9	(0.0:27.3)	
Sex					
Male	115	(51.1%)	1.6	(0.0:18.1)	p = 0.09
Female	110	(48.9%)	0.4	(0.0:27.3)	
Missing	0				
Anatomic site					
Trunk	53	(26.2%)	2.4	(0.0:27.3)	**p < 0.001**
Members	50	(24.8%)	0.0	(0.0:14.4)	
Head	59	(29.2%)	3.7	(0.0:18.7)	
Extremity	40	(19.8%)	0.0	(0.0:5.5)	
Missing	23				
Type					
Dubreuilh	47	(21.6%)	3.9	(0.0:19.4)	**p < 0.001**
SSM	100	(45.9%)	0.8	(0.0:27.3)	
Acral-lentiginous	28	(12.8%)	0.0	(0.0:4.6)	
Others	43	(18.7%)	0.5	(0.0:18.1)	
Missing	7				
Regression					
No	171	(79.2%)			
Yes	45	(20.8%)	0.6	(0.0:27.3)	**p < 0.01**
Missing	9		3.9	(0.0:19.4)	
Tumor ulceration					
No	190	(88.4%)	1.0	(0.0:27.3)	p = 0.41
Yes	25	(11.6%)	0.8	(0.0:13.0)	
Missing	10				
Breslow thickness					
≤ 1 mm	120	(57.1%)	2.6	(0.0:27.3)	**p < 0.001**
1.01–2 mm	34	(16.2%)	1.4	(0.0:10.6)	
> 2 mm	56	(26.7%)	0.1	(0.0:8.7)	
Missing	15				
Clark level					
I–II	80	(36.9%)	2.8	(0.0:27.3)	**p < 0.001**
III	60	(27.6%)	1.3	(0.0:18.7)	
IV–V	77	(35.5%)	0.1	(0.0:19.4)	
Missing	8				
Lymph node invasion					
No	53	(69.7%)	0.8	(0.0:18.1)	p = 0.11
Yes	23	(30.3%)	0.1	(0.0:5.1)	
Missing	0				

(T_{regs}) suppress anti-tumor immune response and their presence has been associated with poor clinical outcome in many cancers.[23] We asked whether the presence of tumor HEVs could impact the density of Foxp3⁺ T-cell infiltrating melanomas. Immunofluorescence staining against Foxp3 on several melanoma tumor sections revealed that the presence of tumor infiltrating Foxp3⁺ CD3⁺ T cells in melanomas is independent of HEV presence (**Fig. 5A**). T_{reg}/T-cell ratio is a crucial parameter defining T_{reg} suppression in melanoma[24] so we evaluated the density of Foxp3⁺ T cells within lymphoid infiltrates surrounding melanoma lesions (**Fig. 5B**). We did not observe any correlation between HEVs and Foxp3⁺ cell densities (**Fig. 5C**), nor

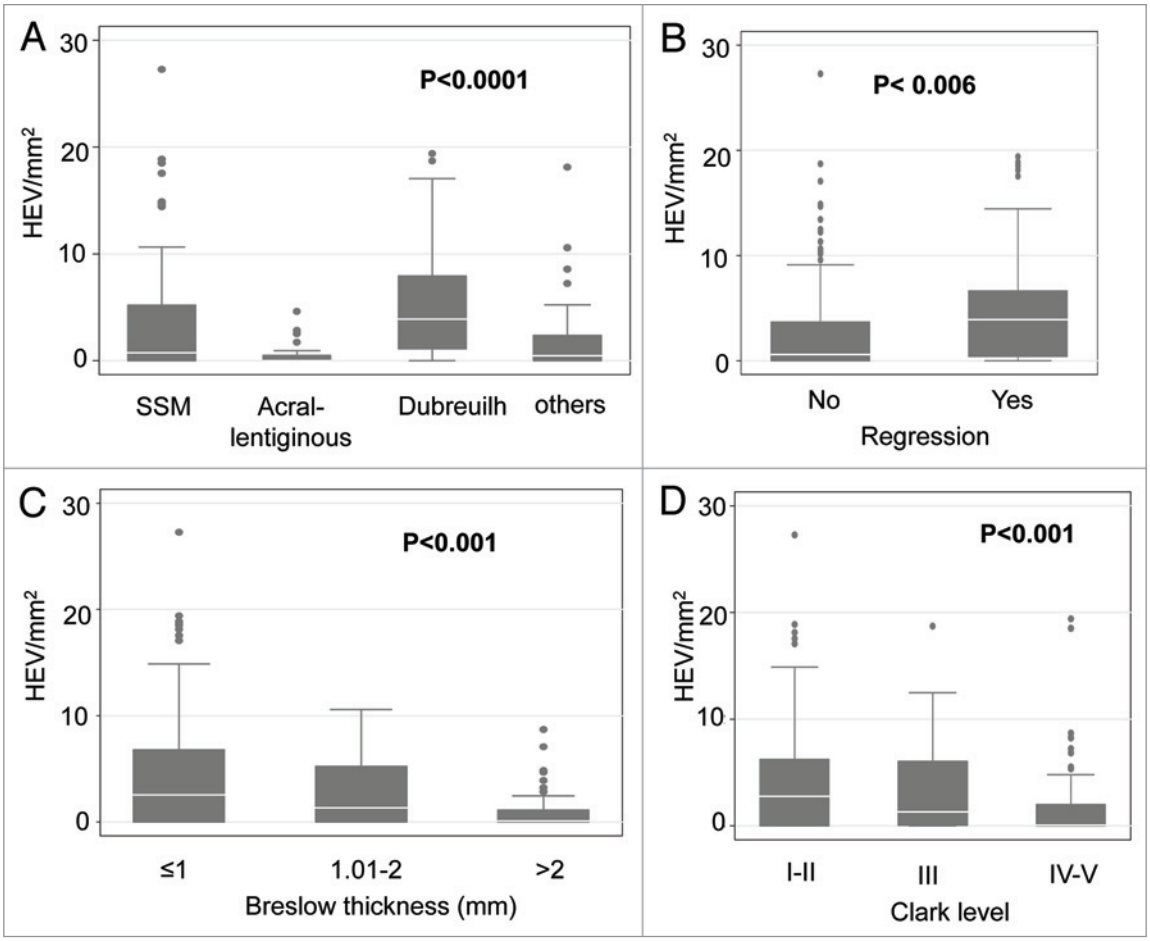

Figure 2. The density of tumor HEVs correlates with clinical characteristics and prognostic biomarkers of primary melanoma. The clinical characteristics and prognostic biomarkers of 225 primary melanomas were analyzed according to the density of HEVs. Significant differences in the density of tumor HEVs were found between patients classified according to melanoma histologic types (**A**), tumor regression (**B**), Breslow thickness (**C**) and Clark level of invasion (**D**). The line in the center of each box represents the median value of the distribution, and the upper and lower ends of the box are the upper and lower quartiles, respectively. Comparisons between groups were performed using the Kruskal-Wallis test.

significant differences in Foxp3⁺ cells densities between samples with a low or a high density of HEVs (**Fig. 5D**). These results demonstrate that although tumor HEVs were correlated with the degree of T-lymphocyte infiltration in melanoma lesions, they had no influence on the densities of T_{regs} in these tumors.

Melanoma tumor HEVs are associated with expression of specific chemokines, chemokine receptors and T_H1 genes. Chemokines orchestrate the trafficking and the correct positioning of immune populations in the different organs of the body. Given the strong association between HEVs and TILs in melanoma, we sought to determine chemokines associated with tumor HEVs in melanoma tumors by qRT-PCR analysis on mRNA extracted from 14 paraffin embedded formalin fixed melanoma samples containing HEVs (HEV^+, n = 7) or not (HEV^-, n = 7). We observed that transcripts coding for chemokines implicated in effector memory T-cell migration into peripheral tissues (*CCL5, CXCL9, CXCL10* and *CXCL11*) were significantly upregulated in melanomas with HEVs (**Fig. 6A**). CXCR3, the receptor for chemokines CXCL9–11 was also overexpressed in HEV^+ melanomas. Genes encoding chemokines mediating naïve T- and B-lymphocyte recruitment into secondary lymphoid organs (*CCL19, CCL21* and *CXCL13*) were also significantly overexpressed in melanomas with HEVs. In contrast, chemokines *CCL2* and *CXCL12* which drive migration of monocytes were highly expressed in melanoma tissue samples independently of HEV presence (**Fig. 6A**). *CCR7* and *L-selectin (Lsel)* which allow naïve lymphocyte migration through HEVs were also strongly overexpressed in HEV^+ melanomas (**Fig. 6A**). These results suggest that HEVs may support naïve T-cell infiltration into melanomas. Immunofluorescence staining against naive lymphocyte marker CD45RA confirmed the presence of some $CD45RA^+$ naïve T cells around HEVs (**Fig. 6B**). Nevertheless, most TILs located around HEVs in melanomas had a $CD45RO^+$ memory phenotype (**Fig. 4B**). We analyzed expression of genes associated with T-helper (T_H) cell orientation in HEV^+ and HEV^- melanoma samples in order to better define effector T-cell responses associated with HEV presence in melanoma. We observed that genes related to T_H1 immune orientation (*TBX21, IFNG*) were significantly upregulated in melanomas with HEVs whereas expression of genes encoding cytokines associated with T_H2, T_H17 and T_{regs} (*IL4, IL17A, IL-10 and TGFB1*) was not significantly modified (**Fig. 6C**).

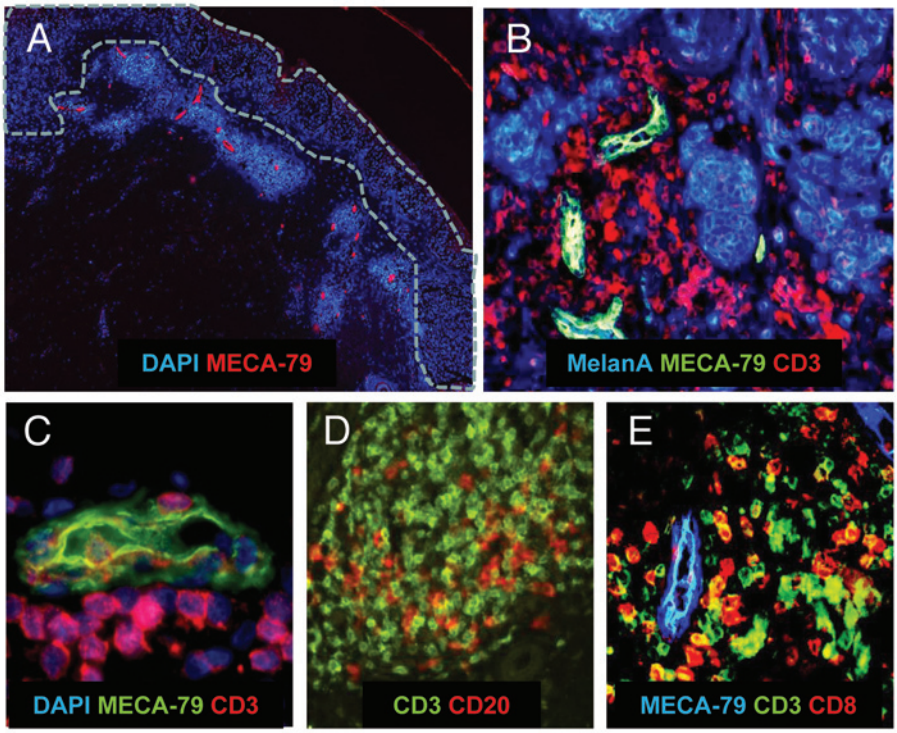

Figure 3. Phenotypic characterization of immune populations associated with HEV blood vessels in melanoma tumors. (**A**) Immune infiltrates are located around MECA-79$^+$ HEV (red)-rich areas of melanoma lesions (dashed area). (**B**) MECA-79$^+$ HEVs (green) are surrounded by numerous CD3$^+$ T lymphocytes (red) that infiltrate melan-A$^+$ tumors (blue). (**C**) CD3$^+$ T cells (red) are seen attached to the luminal surface of MECA-79$^+$ HEV endothelial cells (green) and extravasating through the vessel wall. (**D**) HEVs are present in tumor areas infiltrated mainly by CD3$^+$ T cells (green) and CD20$^+$ B cells (red). (**E**) A considerable fraction of CD3$^+$ T cells (green) surrounding MECA-79$^+$ HEVs (blue) are CD8$^+$ T cytotoxic T cells (red).

The density of tumor HEVs is correlated with the number of DC-LAMP$^+$ dendritic cell clusters. We recently demonstrated that HEV blood vessels in mouse peripheral lymph nodes are maintained by dendritic cells (DCs).[25] To examine a potential link between the presence of DCs and tumor HEVs in melanoma tumors, we performed immunofluorescence and immunohistochemical staining of 30 melanoma tumor sections with antibodies against Fascin and DC-LAMP, two markers of mature DCs. We observed DCs clusters in close proximity to MECA-79$^+$ HEVs in lymphoid infiltrates surrounding melanoma lesions (**Fig. 7A and B**). The amount of DC-LAMP$^+$ infiltrating cells was evaluated through optical grading (grade 1, 2, 3 for low, intermediate and high number of DC-LAMP$^+$ cells) and through the quantification of DC-LAMP$^+$ DCs cluster within tumor areas. We found that the density of tumor HEVs was highly correlated with both DC-LAMP grade (Spearman $r = 0.74$ $p < 0.001$) and number of DC-LAMP$^+$ cell clusters (Spearman $r = 0.72$ $p < 0.001$). The density of HEVs was significantly higher in melanomas with high numbers of DC-LAMP$^+$ tumor infiltrating cells (**Fig. 7C**). Conversely, tumor sections with a high density of HEVs contained higher numbers of DC-LAMP$^+$ clusters than tumors with a low density of HEVs (**Fig. 7D**). Altogether, these results indicate that the presence of tumor HEVs is correlated with the number of DC-LAMP$^+$ DC clusters in the melanoma lesions.

Discussion

Despite the critical role played by immunity in malignant melanoma prognosis[26] and therapeutic response,[10] the mechanisms governing lymphocyte recruitment into melanoma tumors remain poorly defined. In this study, using a cohort of 225 primary melanomas, we provide strong evidence that HEV blood vessels represent major gateways for both T- (effector and naïve) and B-lymphocyte infiltration into melanoma lesions.

T_H1 adaptive immune responses are required for effective anti-tumor immunity[4,27] and T_H1 cytokines have been associated with regressing melanoma.[28,29] Our results demonstrating that tumor HEVs are associated with expression of genes (CXCR3, IFNG and TBX21) and chemokines (CXCL9–11) related to T_H1 effector T cells in melanoma samples suggest that HEV density could represent a crucial determinant of effector T_H1 lymphocyte infiltration into melanoma lesions. At the opposite, Foxp3$^+$ regulatory T cells (T_{regs}) favor immune escape[30] and have been associated with adverse clinical outcome in a variety of malignancies.[31,32] We evaluated the density of T_{regs} within lymphoid infiltrates and found no statistical differences between melanomas with or without HEVs, suggesting that tumor HEVs do not stimulate preferential accumulation of T_{regs} within tumor stroma. In agreement with these results, expression levels of TGFβ and IL-10, two cytokines associated with immune suppression, were not statistically different between HEV$^+$ and HEV$^-$ melanomas.

We observed the presence of CD45RA$^+$ naïve T lymphocytes around HEVs within tumor stroma and HEV$^+$ melanomas were associated with overexpression of chemokines (CCL19, CCL21) and receptors (CCR7, L-selectin/CD62L) driving extravasation of naïve T lymphocytes into lymphoid organs. These results suggest that tumor HEVs, which express high levels of MECA-79$^+$ sulphated L-selectin ligands, support naïve T-cell recruitment into primary melanoma lesions. Interestingly, de Chaisemartin et al. recently reported a similar association between HEVs, lymphoid chemokines and naïve T-cell infiltration in lung carcinomas.[33] Tumor HEVs may play an important role in anti-tumor immunity by facilitating the priming, activation and differentiation of naïve T cells into effectors at the primary tumor site.[34-37] Priming of naïve T cells directly at the tumor site may bring several benefits: (1) the efficiency and the specificity of

T-cell priming may be improved thanks to the higher antigenic load in situ than in the draining lymph node;[38] (2) a broader repertoire of tumor antigens may be presented to naïve T cells;[39] (3) newly generated effector T cells would not need additional migration steps to reach effector sites. Even if we can't formally prove it, our study supports the possibility that naïve T-cell priming and differentiation may take place within human primary melanomas thanks to the presence of all the critical elements for effective T-cell responses: tumor HEVs and lymphoid chemokines for T-cell migration, mature DCs clusters around HEVs for T-cell stimulation.

Recent melanoma staging recommendations from American Joint Committee on Cancer (AJCC) indicate that Breslow tumor thickness remains the most powerful prognostic factor for localized melanoma overall survival.[22] Our results revealed an inverse correlation between Breslow thickness and HEV density. Indeed T1 melanomas (Breslow ≤ 1 mm) contained statistically more HEVs than T2 (Breslow 1.01–2 mm) and T3–4 (Breslow > 2 mm) melanomas. An inverse correlation was also observed between Clark level of invasion and HEV density demonstrating that HEV density is decreased when melanoma invade deeper through the dermis. Altogether, these results suggest that the density of tumor HEVs could represent an important prognostic biomarker in melanoma. Interestingly, although HEV density correlated with $CD3^+$, $CD8^+$ and $CD20^+$ TILs (**Table S1**), the associations between HEV densities and melanoma prognostic biomarkers (**Table 1**) were stronger than those for TILs (**Tables S2–S4**). The density of tumor HEVs, which correlates with the presence of mDCs and both effector and naïve T-cell infiltration, may thus represent a more powerful immune marker than different TILs sub-populations. Future studies will have to determine whether HEV density significantly impacts melanoma patient's survival and represents a valuable independent marker for melanoma classification and medical care.

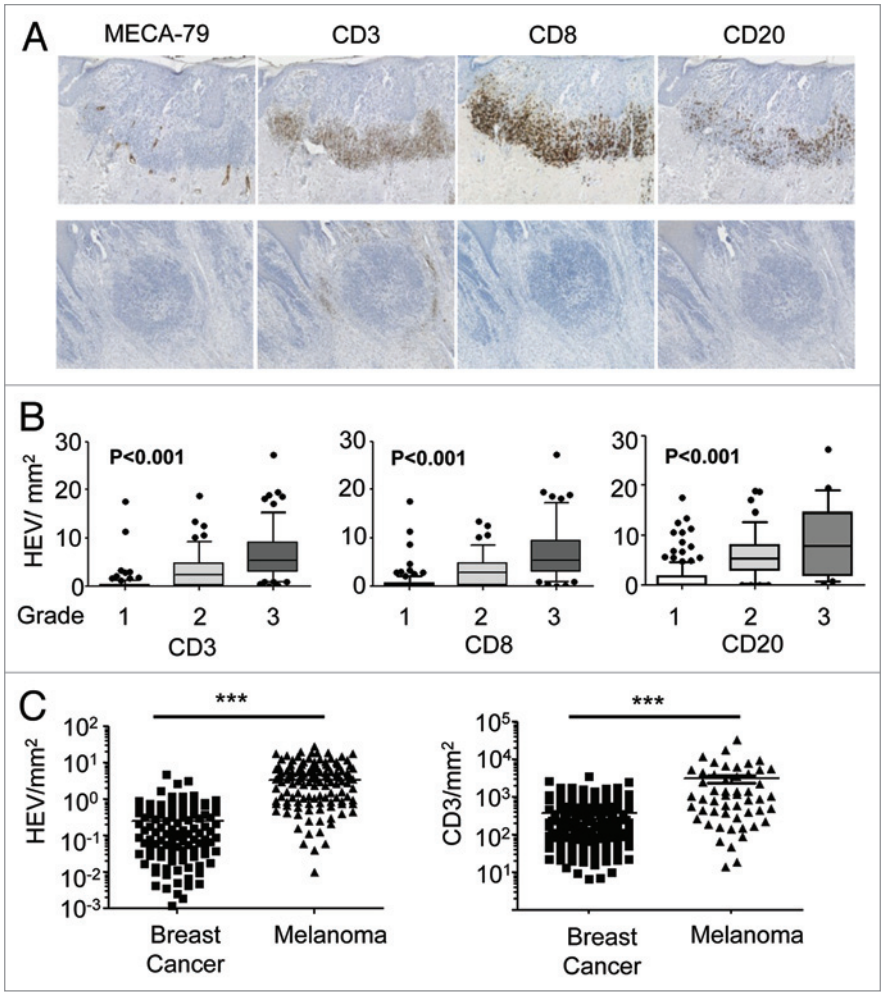

Figure 4. The density of tumor HEVs predicts lymphocyte infiltration in melanoma. (**A and B**) Consecutive tumor sections from 225 melanomas were analyzed by immunohistochemistry with MECA-79, anti-CD3, anti-CD8 and anti-CD20 antibodies. The number of $CD3^+$, $CD8^+$ and $CD20^+$ TILs was quantified by semi quantitative optical grading (grade 1–3 for low, moderate and high density of positive cells). (**A**) Representative pictures showing HEVs and the indicated immune populations in tumors with (upper part) and without (lower part) tumor HEVs. (**B**) Graphs showing the density of HEVs in melanoma tumors according to the density of $CD3^+$, $CD8^+$ and $CD20^+$ TILs. $p < 0.001$; Kruskal-wallis test. (**C**) Graphs showing the densities of HEVs and $CD3^+$ T cells (lower graph) in melanomas (n = 225) and invasive breast tumors (n = 146). ***$p < 0.001$; Mann Whitney test.

Melanoma is considered one of the most immunogenic solid tumors and the ideal candidate against which to develop various immunotherapeutic approaches.[40] However, most strategies have obtained limited results. The existence of immune regulatory mechanisms has been suggested to account for immunotherapy failure.[40] The inability of effector immune cells to reach tumor sites also represents a major limit to effective immunotherapy.[16,41] In this study, we provide strong evidence that tumor HEVs represent major gateways for infiltration of both effector T_H1 and naïve T lymphocytes into primary melanoma lesions. These results suggest that it may be possible to improve lymphocyte infiltration into melanomas by increasing the number of HEVs within tumor stroma. Our results revealed a strong correlation between the density of tumor HEVs and the number of DC-LAMP$^+$ mDCs clusters within primary melanoma lesions. This observation suggests that mDCs within melanomas may not only function as antigen presenting cells but may also participate in the induction and/or maintenance of HEVs in the tumor microenvironment, similar to the role of DCs in the maintenance of HEVs from lymphoid organs.[25] Further characterization of the role of DCs in the regulation of HEV blood vessels may lead to novel therapeutic strategies for melanoma and other solid tumors.

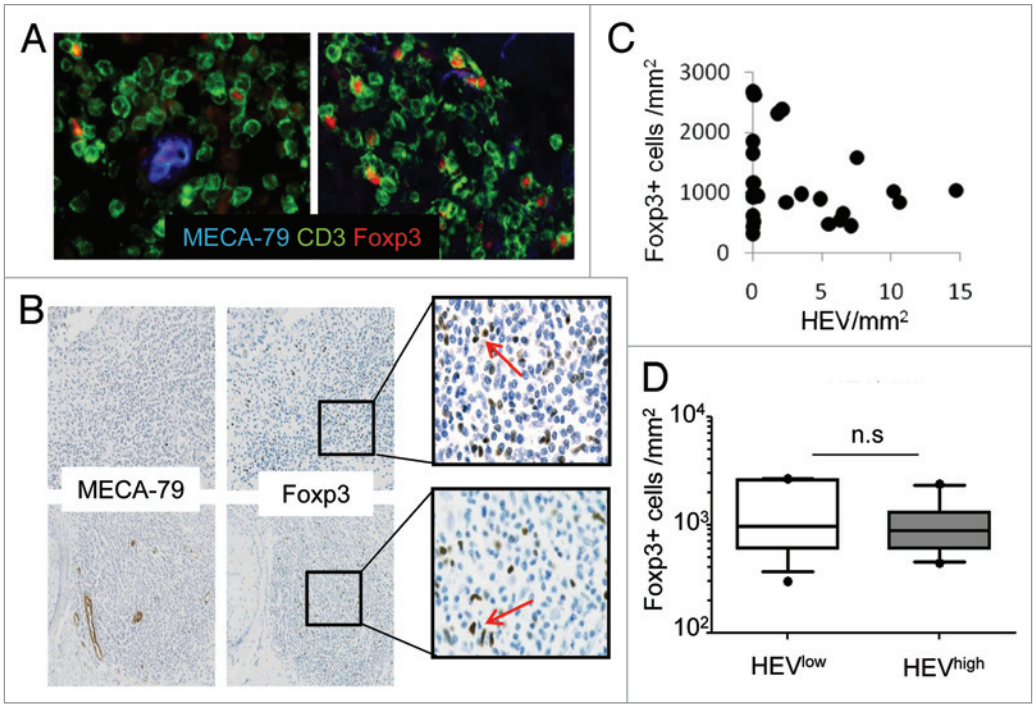

Figure 5. The density of tumor HEVs has no influence on the density of tumor infiltrating Foxp3$^+$ T cells. (**A**) Representative immunofluorescence staining of melanoma tumor sections with the indicated antibodies showing Foxp3$^+$ T cells (red) within T cells infiltrates (green) in melanomas containing MECA-79$^+$ HEVs (blue) or not. (**B**) Consecutive melanoma sections from representative tumors with a high and a low density of MECA-79$^+$ HEVs (n = 30) were stained with anti-Foxp3 antibodies and the density of Foxp3$^+$ cells (red arrow) within melanoma lymphoid stroma was calculated. (**C**) The density of Foxp3$^+$ cells within peri-tumor lymphoid infiltrates is not correlated with the density of tumor HEVs. (**D**) The density of Foxp3$^+$ cells within peri-tumor lymphoid infiltrates is similar in melanomas with a low and a high density of tumor HEVs. n.s $p > 0.05$ Mann Whitney test.

Patients and Methods

Patients. Approval of the study was obtained from the scientific review board of the Institute Claudius Regaud (ICR, Toulouse, France). A cohort of 225 primary melanoma patients operated between 2000 and 2012 in the Institute Claudius Regaud and the CHU Toulouse Purpan were included in this study. The clinical characteristics of the patients are summarized in **Table 1**. The median age of the patients was 65 y and 51% were male. The most common site of melanoma was head (29%) followed by trunk (26%), members (25%) and extremity (20%). The most common melanoma histologic type was SSM (45.9%) followed by Dubreuilh (21.6%) and Acral-lentiginous (12.8%). The median Breslow depth was 0.9 mm. 36.9% of patients had Clark I–II levels, 27.6% Clark III and 35.5% Clark IV–V. Ulceration was present in 12% of patients and tumor regression was observed for 21%. Sentinel lymph node was evaluated for 76 patients among whom 30% had detectable metastasis.

Immunohistochemistry and immunofluorescence staining. Immunohistochemistry was performed on 5-μm consecutive sections from paraffin embedded tumor blocks using a Techmate Horizon slide processor (Dako) as described previously in reference 21. Details of the antibodies, fixatives and antigen retrieval methods used are provided in **Table S5**. Briefly, slides were incubated with primary antibodies for 1 h at room temperature, antigen-antibody complexes were detected using a peroxidase-conjugated polymer backbone coupled to secondary antibody system (EnVision, Dako) and 3,3'-diaminobenzydine chromogen (Dako). For immunofluorescence detection, slides were incubated with fluorochrome-coupled secondary antibodies, diluted in PBS, BSA 1% for 1 h at room temperature and counterstained with DAPI.

Method for cell quantification. Tumor slides stained with MECA-79, anti-CD3, anti-CD8, anti-CD20, anti-Foxp3 and anti-DC-LAMP antibodies were scanned with a high-resolution scanner (NDP slide scanner, Hamamatsu and Panoramic 250 Flash, 3Dhistech). Absolute numbers of MECA-79$^+$ vessels present within the tumor area (mm^2) were quantified for each tumor slide and the densities of tumor HEVs (HEV/mm^2) were calculated. The amount of CD3$^+$, CD20$^+$ and CD8$^+$ infiltrating cells were evaluated by optical grading as described previously in references 8 and 9 (score 1, 2, 3 for absent-low, moderate and high density of positive cells). Automatic cell counts of CD3$^+$ cells were determined for 50 primary melanomas as described previously in reference 21, with image J software (NIH) using a macro designed by R. Poincloux (IPBS) in order to validate optical grading (**Fig. S3**). The density of Foxp3$^+$ cells was calculated by optical counting of positive cells on 5 representative fields within lymphoid infiltrates surrounding melanoma lesions (0.01 mm^2; original magnification 100x). We evaluated the relative amount of DC-LAMP$^+$ infiltrating cells either by optical grading (grade 1–3 for low, intermediate and high number of tumor-infiltrating DC-LAMP$^+$ cells) or by optical quantification of the number and density of DC-LAMP$^+$ cells clusters within melanoma tumor stroma (**Fig. S3**). Quantification

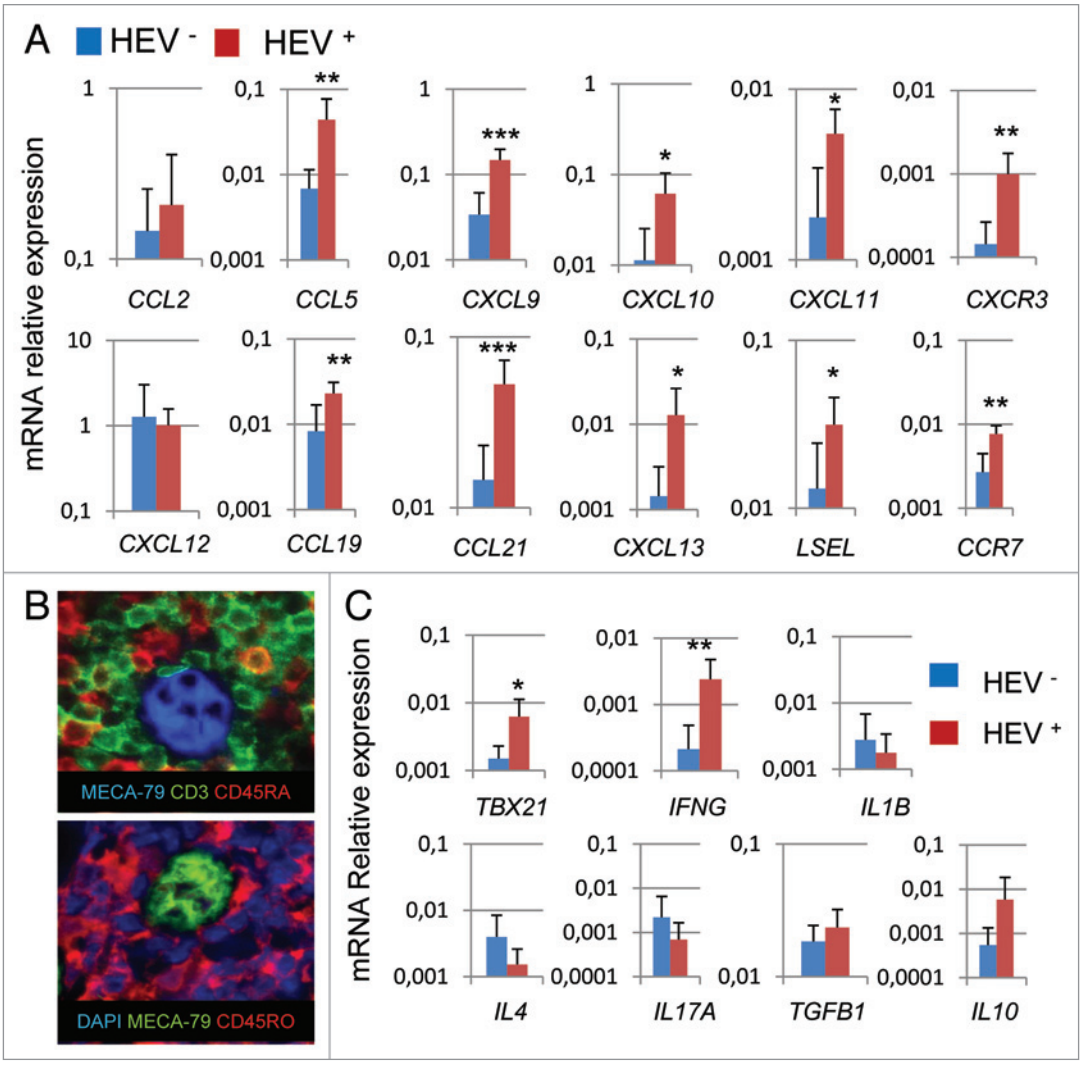

Figure 6. Expression of specific chemokines, chemokine receptors, T_H1 and naïve T cell genes in melanoma tumors containing HEVs. (**A**) Expression of genes related to lymphocyte migration was determined by qRT-PCR in 14 melanoma samples according to the presence of tumor HEVs (7 HEV^+ vs. 7 HEV^-). Relative mRNA expression levels were adjusted to the levels of the housekeeping gene *YWHAZ*, and are represented as mean relative expression (+SD) for HEV^+ (red bars) and HEV^- (blue bars) tumors. (**B**) Representative immunofluorescence staining of melanoma tumor sections with the indicated antibodies showing numerous $CD45RO^+$ lymphocytes and a few $CD45RA^+$ naïve T cells around $MECA\text{-}79^+$ HEVs. (**C**) Expression of genes related to T Helper orientation was determined by qRT-PCR in 14 melanoma samples according to the presence of tumor HEVs (7 HEV^+ vs. 7 HEV^-). The levels are represented as mean relative expression (+SD) for HEV^+ (red bars) and HEV^- (blue bars) tumors. *p < 0.05, **p < 0.01, ***p < 0.001; Mann Whitney test.

of vessels and immune scoring were performed by two independent observers (L.M. and S.L.).

Quantitative RT-PCR. An RNeasy FFPE isolation kit was used to isolate total RNA (Qiagen) from 14 paraffin-embedded melanoma tumor samples with or without tumor HEVs (detected by MECA-79 staining on adjacent paraffin embedded tumor sections). The integrity and the quantity of the RNA were evaluated using a bioanalyzer-2100 (Agilent Technologies). cDNA was prepared by reverse-transcription using superscript VILO cDNA Synthesis Kit (Invitrogen). RT-PCR experiments were performed using Power SYBR Green mix with an ABI PRISM 7300HT (Applied Biosystems) according to manufacturer instructions. All reactions were done in duplicate and normalized to the expression of the house keeping gene *YWHAZ*. For each gene, relative expression was calculated by the Δ cycling threshold (CT) method as $2^{-(\Delta CTsample)}$ with $\Delta CTsample = CT_{gene} - CT_{YWHAZ}$.

Statistical analysis. Data were summarized by frequency and percentage for categorical variables and by median and range for continuous variables. Comparisons between groups were performed using the Kruskal-Wallis test for continuous variables. Correlations between continuous variables were evaluated using Spearman's rank correlation test. All p values reported were two-sided. For all statistical tests, differences were considered significant at the 5% level. Statistical analyses were performed using the STATA 11.0 (STATA Corp.) software.

Disclosure of Potential Conflicts of Interest

No potential conflicts of interest were disclosed.

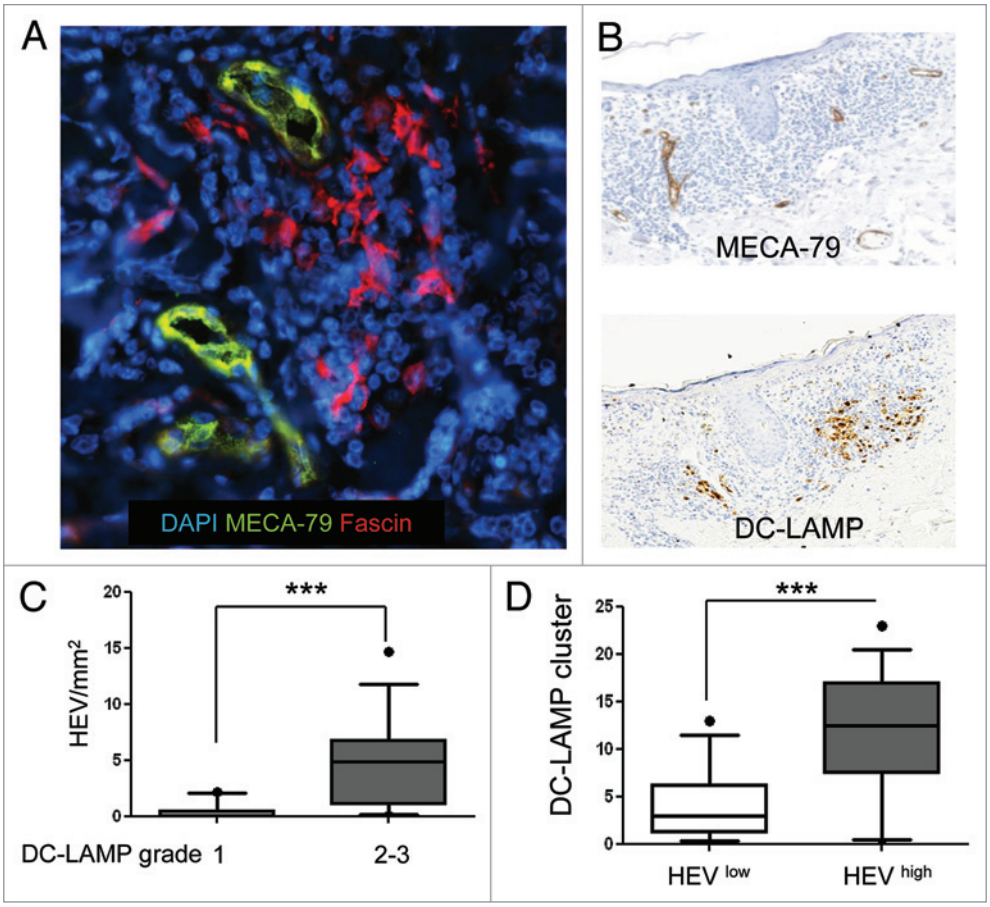

Figure 7. The presence of tumor HEVs in melanoma lesions is correlated with the number of DC-LAMP⁺ DCs clusters. (**A**) Immunofluorescence staining showing Fascin⁺ DCs (red) around MECA-79⁺ HEVs (green) within melanoma lymphoid infiltrates. (**B–D**) Consecutive melanoma sections from tumors with a high and a low density of MECA-79⁺ HEVs (n = 30) were stained with antibodies directed against DC-LAMP and the number of DC-LAMP⁺ cells clusters was calculated. (**B**) Representative picture showing MECA-79⁺ HEVs in a tumor area infiltrated by DC-LAMP⁺ DCs. (**C**) The density of MECA-79⁺ HEVs is significantly higher in melanomas with a high amount of DC-LAMP⁺ infiltrating DCs (grades 2 and 3) as compared with melanomas with a low amount of DC-LAMP⁺ infiltrating DCs (grade 1). (**D**) The number of DC-LAMP⁺ DCs clusters is significantly higher in melanomas with a high density of tumor HEVs. ***p < 0.001; Mann Whitney test.

Acknowledgements

L.M. designed research, performed research, analyzed data and wrote the paper; S.L.G. performed research and analyzed data; T.F. analyzed data; L.L. designed research; N.M. designed research; P.R. designed research; I.G. designed research and analyzed data; J.P.G. designed research, analyzed data and wrote the paper. This work was supported by grants from Fondation RITC and Région Midi-Pyrénées (to J.P.G.), GR-ICR (to I.G.), Association pour la Recherche Contre le Cancer (Programme ARC to J.P.G.) and Ligue Nationale Contre le Cancer (Equipe Labelisée Ligue 2009 to J.P.G., post-doctoral Fellowship to L.M.). We are grateful to Dr Veronique Maisongrosse and all the members of the ICR Anatomopathology Service for their help. We thank the Biological Resource Center (CRB) of the ICR for providing melanoma tumor samples. We thank Renaud Poincloux for designing the lymphocyte count macro. We thank Chamroeun SAR from the Montpellier Rio Imaging facility for access to the high-resolution scanner.

Supplemental Materials

Supplemental materials may be found here:
www.landesbioscience.com/journals/oncoimmunology/article/20492/

References

1. MacKie RM, Hauschild A, Eggermont AM. Epidemiology of invasive cutaneous melanoma. Ann Oncol 2009; 20:1-7; PMID:19617292; http://dx.doi.org/10.1093/annonc/mdp252.
2. Disis ML. Immune regulation of cancer. J Clin Oncol 2010; 28:4531-8; PMID:20516428; http://dx.doi.org/10.1200/JCO.2009.27.2146.
3. Pagès F, Berger A, Camus M, Sanchez-Cabo F, Costes A, Molidor R, et al. Effector memory T cells, early metastasis and survival in colorectal cancer. N Engl J Med 2005; 353:2654-66; PMID:16371631; http://dx.doi.org/10.1056/NEJMoa051424.
4. Galon J, Costes A, Sanchez-Cabo F, Kirilovsky A, Mlecnik B, Lagorce-Pagès C, et al. Type, density and location of immune cells within human colorectal tumors predict clinical outcome. Science 2006; 313:1960-4; PMID:17008531; http://dx.doi.org/10.1126/science.1129139.
5. Zhang L, Conejo-Garcia JR, Katsaros D, Gimotty PA, Massobrio M, Regnani G, et al. Intratumoral T cells, recurrence and survival in epithelial ovarian cancer. N Engl J Med 2003; 348:203-13; PMID:12529460; http://dx.doi.org/10.1056/NEJMoa020177.
6. Fridman WH, Galon J, Pagès F, Tartour E, Sautès-Fridman C, Kroemer G. Prognostic and predictive impact of intra- and peritumoral immune infiltrates. Cancer Res 2011; 71:5601-5; PMID:21846822; http://dx.doi.org/10.1158/0008-5472.CAN-11-1316.

7. Taylor RC, Patel A, Panageas KS, Busam KJ, Brady MS. Tumor-infiltrating lymphocytes predict sentinel lymph node positivity in patients with cutaneous melanoma. J Clin Oncol 2007; 25:869-75; PMID:17327608; http://dx.doi.org/10.1200/JCO.2006.08.9755.
8. Clark WH Jr, Elder DE, Guerry D, 4th, Braitman LE, Trock BJ, Schultz D, et al. Model predicting survival in stage I melanoma based on tumor progression. J Natl Cancer Inst 1989; 81:1893-904; PMID:2593166; http://dx.doi.org/10.1093/jnci/81.24.1893.
9. Clemente CG, Mihm MC Jr, Bufalino R, Zurrida S, Collini P, Cascinelli N. Prognostic value of tumor infiltrating lymphocytes in the vertical growth phase of primary cutaneous melanoma. Cancer 1996; 77:1303-10; PMID:8608507; http://dx.doi.org/10.1002/(SICI)1097-0142(19960401)77:7<1303::AID-CNCR12>3.0.CO;2-5.
10. Robert C, Thomas L, Bondarenko I, O'Day S, M D JW, Garbe C, et al. Ipilimumab plus dacarbazine for previously untreated metastatic melanoma. N Engl J Med 2011; 364:2517-26; PMID:21639810; http://dx.doi.org/10.1056/NEJMoa1104621.
11. Dudley ME, Wunderlich JR, Yang JC, Sherry RM, Topalian SL, Restifo NP, et al. Adoptive cell transfer therapy following non-myeloablative but lymphodepleting chemotherapy for the treatment of patients with refractory metastatic melanoma. J Clin Oncol 2005; 23:2346-57; PMID:15800326; http://dx.doi.org/10.1200/JCO.2005.00.240.
12. Moschos SJ, Edington HD, Land SR, Rao UN, Jukic D, Shipe-Spotloe J, et al. Neoadjuvant treatment of regional stage IIIB melanoma with high-dose interferon alfa-2b induces objective tumor regression in association with modulation of tumor infiltrating host cellular immune responses. J Clin Oncol 2006; 24:3164-71; PMID:16809739; http://dx.doi.org/10.1200/JCO.2005.05.2498.
13. Tarhini AA, Kirkwood JM, Gooding WE, Cai C, Agarwala SS. Durable complete responses with high-dose bolus interleukin-2 in patients with metastatic melanoma who have experienced progression after biochemotherapy. J Clin Oncol 2007; 25:3802-7; PMID:17761969; http://dx.doi.org/10.1200/JCO.2006.10.2822.
14. Cipponi A, Wieers G, van Baren N, Coulie PG. Tumor-infiltrating lymphocytes: apparently good for melanoma patients. But why? Cancer Immunol Immunother 2011; 60:1153-60; PMID:21553145; http://dx.doi.org/10.1007/s00262-011-1026-2.
15. Girard JP, Springer TA. High endothelial venules (HEVs): specialized endothelium for lymphocyte migration. Immunol Today 1995; 16:449-57; PMID:7546210; http://dx.doi.org/10.1016/0167-5699(95)80023-9.
16. Buckanovich RJ, Facciabene A, Kim S, Benencia F, Sasaroli D, Balint K, et al. Endothelin B receptor mediates the endothelial barrier to T cell homing to tumors and disables immune therapy. Nat Med 2008; 14:28-36; PMID:18157142; http://dx.doi.org/10.1038/nm1699.
17. Weishaupt C, Munoz KN, Buzney E, Kupper TS, Fuhlbrigge RC. T-cell distribution and adhesion receptor expression in metastatic melanoma. Clin Cancer Res 2007; 13:2549-56; PMID:17473183; http://dx.doi.org/10.1158/1078-0432.CCR-06-2450.
18. von Andrian UH, Mempel TR. Homing and cellular traffic in lymph nodes. Nat Rev Immunol 2003; 3:867-78; PMID:14668803; http://dx.doi.org/10.1038/nri1222.
19. Aloisi F, Pujol-Borrell R. Lymphoid neogenesis in chronic inflammatory diseases. Nat Rev Immunol 2006; 6:205-17; PMID:16498451; http://dx.doi.org/10.1038/nri1786.
20. Kobayashi M, Mitoma J, Nakamura N, Katsuyama T, Nakayama J, Fukuda M. Induction of peripheral lymph node addressin in human gastric mucosa infected by *Helicobacter pylori*. Proc Natl Acad Sci USA 2004; 101:17807-12; PMID:15591109; http://dx.doi.org/10.1073/pnas.0407503101.
21. Martinet L, Garrido I, Filleron T, Le Guellec S, Bellard E, Fournie JJ, et al. Human solid tumors contain high endothelial venules: association with T- and B-lymphocyte infiltration and favorable prognosis in breast cancer. Cancer Res 2011; 71:5678-87; PMID:21846823; http://dx.doi.org/10.1158/0008-5472.CAN-11-0431.
22. Balch CM, Gershenwald JE, Soong SJ, Thompson JF, Atkins MB, Byrd DR, et al. Final version of 2009 AJCC melanoma staging and classification. J Clin Oncol 2009; 27:6199-206; PMID:19917835; http://dx.doi.org/10.1200/JCO.2009.23.4799.
23. Jacobs JF, Nierkens S, Figdor CG, de Vries IJ, Adema GJ. Regulatory T cells in melanoma: the final hurdle towards effective immunotherapy? Lancet Oncol 2012; 13:32-42; PMID:22225723; http://dx.doi.org/10.1016/S1470-2045(11)70155-3.
24. Quezada SA, Peggs KS, Curran MA, Allison JP. CTLA4 blockade and GM-CSF combination immunotherapy alters the intratumor balance of effector and regulatory T cells. J Clin Invest 2006; 116:1935-45; PMID:16778987; http://dx.doi.org/10.1172/JCI27745.
25. Moussion C, Girard JP. Dendritic cells control lymphocyte entry to lymph nodes through high endothelial venules. Nature 2011; 479:542-6; PMID:22080953; http://dx.doi.org/10.1038/nature10540.
26. Oble DA, Loewe R, Yu P, Mihm MC Jr. Focus on TILs: prognostic significance of tumor infiltrating lymphocytes in human melanoma. Cancer Immun 2009; 9:3; PMID:19338264.
27. Vesely MD, Kershaw MH, Schreiber RD, Smyth MJ. Natural innate and adaptive immunity to cancer. Annu Rev Immunol 2011; 29:235-71; PMID:21219185; http://dx.doi.org/10.1146/annurev-immunol-031210-101324.
28. Lowes MA, Bishop GA, Crotty K, Barnetson RS, Halliday GM. T helper 1 cytokine mRNA is increased in spontaneously regressing primary melanomas. J Invest Dermatol 1997; 108:914-9; PMID:9182821; http://dx.doi.org/10.1111/1523-747.ep12292705.
29. Wagner SN, Schultewolter T, Wagner C, Briedigkeit L, Becker JC, Kwasnicka HM, et al. Immune response against human primary malignant melanoma: a distinct cytokine mRNA profile associated with spontaneous regression. Lab Invest 1998; 78:541-50; PMID:9605179.
30. Zou W. Regulatory T cells, tumour immunity and immunotherapy. Nat Rev Immunol 2006; 6:295-307; PMID:16557261; http://dx.doi.org/10.1038/nri1806.
31. Bates GJ, Fox SB, Han C, Leek RD, Garcia JF, Harris AL, et al. Quantification of regulatory T cells enables the identification of high-risk breast cancer patients and those at risk of late relapse. J Clin Oncol 2006; 24:5373-80; PMID:17135638; http://dx.doi.org/10.1200/JCO.2006.05.9584.
32. Curiel TJ, Coukos G, Zou L, Alvarez X, Cheng P, Mottram P, et al. Specific recruitment of regulatory T cells in ovarian carcinoma fosters immune privilege and predicts reduced survival. Nat Med 2004; 10:942-9; PMID:15322536; http://dx.doi.org/10.1038/nm1093.
33. de Chaisemartin L, Goc J, Damotte D, Validire P, Magdeleinat P, Alifano M, et al. Characterization of chemokines and adhesion molecules associated with T cell presence in tertiary lymphoid structures in human lung cancer. Cancer Res 2011; 71:6391-9; PMID:21900403; http://dx.doi.org/10.1158/0008-5472.CAN-11-0952.
34. Thompson ED, Enriquez HL, Fu YX, Engelhard VH. Tumor masses support naive T cell infiltration, activation and differentiation into effectors. J Exp Med 2010; 207:1791-804; PMID:20660615; http://dx.doi.org/10.1084/jem.20092454.
35. Schrama D, thor Straten P, Fischer WH, McLellan AD, Bröcker EB, Reisfeld RA, et al. Targeting of lymphotoxin-alpha to the tumor elicits an efficient immune response associated with induction of peripheral lymphoid-like tissue. Immunity 2001; 14:111-21; PMID:11239444; http://dx.doi.org/10.1016/S1074-7613(01)00094-2.
36. Yu P, Lee Y, Liu W, Chin RK, Wang J, Wang Y, et al. Priming of naive T cells inside tumors leads to eradication of established tumors. Nat Immunol 2004; 5:141-9; PMID:14704792; http://dx.doi.org/10.1038/ni1029.
37. Yu P, Lee Y, Wang Y, Liu X, Auh S, Gajewski TF, et al. Targeting the primary tumor to generate CTL for the effective eradication of spontaneous metastases. J Immunol 2007; 179:1960-8; PMID:17641063.
38. Spiotto MT, Yu P, Rowley DA, Nishimura MI, Meredith SC, Gajewski TF, et al. Increasing tumor antigen expression overcomes "ignorance" to solid tumors via crosspresentation by bone marrow-derived stromal cells. Immunity 2002; 17:737-47; PMID:12479820; http://dx.doi.org/10.1016/S1074-7613(02)00480-6.
39. Bai XF, Liu J, Li O, Zheng P, Liu Y. Antigenic drift as a mechanism for tumor evasion of destruction by cytolytic T lymphocytes. J Clin Invest 2003; 111:1487-96; PMID:12750398.
40. Eggermont AM. Immunotherapy: Vaccine trials in melanoma—time for reflection. Nat Rev Clin Oncol 2009; 6:256-8; PMID:19390551; http://dx.doi.org/10.1038/nrclinonc.2009.42.
41. Chen Q, Wang WC, Evans SS. Tumor microvasculature as a barrier to antitumor immunity. Cancer Immunol Immunother 2003; 52:670-9; PMID:12920482; http://dx.doi.org/10.1007/s00262-003-0425-4.